

UTILITY OF DIFFUSION WEIGHTED IMAGING IN DIFFERENTIATING BENIGN AND MALIGNANT CERVICAL LYMPH NODES

Dr. Abishek D ¹, Dr. Aadithiyar Sekar ^{2*}, Dr. Aashika Parveen Amir ³ and Dr. Lathika Shetty ⁴

¹ Senior Resident, Department of Radio Diagnosis, K.S. Hegde Medical College, Derlakatte, Mangaluru, Karnataka, India.

² Senior Resident, Department of Radio Diagnosis, Saveetha Medical College and Hospital, Thandalam, Chennai, Tamilnadu, India. *Corresponding Author

³ Post Graduate, Department of Radio Diagnosis, Saveetha Medical College and Hospital, Thandalam, Chennai, Tamilnadu, India.

⁴ Professor, Department of Radio Diagnosis, K.S. Hegde Medical College, Derlakatte, Mangaluru, Karnataka, India.

DOI: [10.5281/zenodo.12567366](https://doi.org/10.5281/zenodo.12567366)

Abstract

Background: Detection of cervical lymph nodes and their differentiation into benign or malignant is important especially in patients with head and neck cancer for staging, treatment planning and follow-up of cancer. This study aims to evaluate the role of DWI in differentiating benign and malignant cervical lymph nodes by evaluating the ADC values in different malignant histopathologies. **Methods and Materials:** A observational study was conducted in the department of Radiodiagnosis in a tertiary care hospital over a period of one and half year. 47 subjects with cervical lymphadenopathy were included in the study after fulfilling the inclusion and exclusion criteria. ADC maps were reconstructed for all patients and ADC values were calculated for each lymph node. DWI was performed using a single-shot echo-planar MRI sequence with b values of 0,500 and 1000s/mm². Imaging results were correlated with histopathological diagnosis. **Results:** Cervical lymph node enlargement was secondary to metastases from squamous cell carcinomas, metastasis from small cell carcinoma of lung, metastasis from medullary carcinoma thyroid, NHL, HL, reactive lymphadenitis, tuberculosis and kichu lymphadenitis. The mean ADC values were $0.75 \pm 0.11 \times 10^{-3} \text{mm}^2/\text{s}$ for metastatic lymph nodes, $0.68 \pm 0.09 \times 10^{-3} \text{mm}^2/\text{s}$ for lymphomatous nodes and $1.11 \pm 0.15 \times 10^{-3} \text{mm}^2/\text{s}$ for benign cervical lymph nodes. ADC values of malignant lymph nodes were significantly lower than ADC values of benign lymph nodes. The ADC value of the metastatic lymph node varied according to degree of differentiation. Poorly differentiated metastatic lymph nodes showed lower ADC values than moderately differentiated lesions. Using a threshold ADC value of $0.95 \times 10^{-3} \text{mm}^2/\text{s}$ 93.6% of lesions were correctly classified as benign or malignant. **Conclusion:** Evaluation of lymph nodes by MRI can help the radiologist to differentiate benign and malignant lymph nodes. However, histopathological diagnosis will remain mainstay in differentiating benign and malignant lymph nodes. DW-MRI with ADC mapping is a promising technique that can differentiate malignant from benign lymph nodes. DWI can be preferred as a non-invasive method for patients with enlarged cervical lymph nodes enabling earlier diagnosis and treatment planning.

INTRODUCTION

The accurate detection and classification of cervical lymph nodes as benign or malignant is crucial for effective staging, treatment planning, and cancer monitoring, particularly in patients with head and neck cancer. Traditional imaging methods rely on morphological features such as the maximum short axial diameter, presence of necrosis, loss of lymph node hilum, heterogeneous enhancement, and perinodal infiltration. However, these criteria often fail to differentiate between benign and malignant lymph nodes effectively.

While ultrasound (US), computed tomography (CT), and magnetic resonance imaging (MRI) can identify enlarged lymph nodes, they struggle to distinguish between benign and malignant types. Metabolic imaging techniques like single photon emission

computed tomography and positron emission tomography can aid in this differentiation, but they have limitations such as low spatial resolution and variable physiological uptake. Fine needle aspiration cytology (FNAC) guided by ultrasound is another method, but it's invasive and operator-dependent. Although conventional MRI is not significantly better than CT in this regard, the use of ultrasmall superparamagnetic iron oxide particles (USPIO) as MRI contrast agents shows promise in lymph node staging. However, this approach requires two consecutive scans and poses risks of adverse effects. Diffusion weighted magnetic resonance imaging (DW-MRI) emerges as a promising non-invasive functional technique for this purpose. DW-MRI analyzes tissue microstructure by measuring the random diffusion of water molecules. Initially developed for intracranial evaluations, advancements in MRI technology have extended its applicability to extracranial regions.

The primary factor influencing diffusion in tissues is cellularity. Malignant cells, characterized by increased cell density, nucleocytoplasmic ratio, and reduced extracellular space, restrict water molecule diffusion more than benign cells. The apparent diffusion coefficient (ADC) map derived from DW-MRI provides a quantitative measure of water diffusion, enabling more precise tissue characterization.

Our study aims to assess the efficacy of DW-MRI in distinguishing between benign and malignant cervical lymph nodes by examining ADC values across various malignant histopathologies. This innovative approach holds promise for improving the accuracy of lymph node classification without the drawbacks associated with current methods.

METHODOLOGY

The study was a hospital-based observational research conducted at a tertiary care centre from April 2021 to September 2022. The objective was to evaluate the efficacy of diffusion weighted magnetic resonance imaging (DW-MRI) in distinguishing benign from malignant cervical lymph nodes, focusing on apparent diffusion coefficient (ADC) values across various malignant histopathologies.

The study population comprised patients undergoing MRI for cervical lymph node masses. Based on a prior studies, the required sample size was determined to be 44 using nMASTER software, with a 5% error margin and a standard deviation (SD) of ADC (malignant and benign) set at 0.135.

Patients eligible for inclusion were those with Histopathologically confirmed malignancy undergoing MRI for staging, those with suspected malignancy later confirmed by histopathological examination (HPE), and those with incidentally detected cervical lymph node masses subsequently proven malignant by HPE. Patients contraindicated for MRI were excluded.

After obtaining Institutional Ethical Committee clearance, informed consent was secured from all participants. MRI scans were performed using a SIEMENS MAGNETOM AVANTO 1.5 TESLA machine, employing various sequences including axial, coronal, and sagittal T1 and T2 weighted spin echo, gradient echo, short tau inversion recovery, and DW sequences.

Data collection involved recording imaging features, calculating ADC values from ADC maps, and gathering clinical, histopathological, and demographic information from patient records. All identifiable information was anonymized prior to analysis.

Data were tabulated using Microsoft Excel 2019 and analyzed using IBM SPSS Statistics Version 23.0. Descriptive statistics, frequency, and percentage analyses were applied for categorical variables, while mean and standard deviation (S.D) were used for continuous variables. The Independent sample t-test was employed to determine significant differences between bivariate samples in independent groups.

The predictive efficacy of ADC in determining malignancy was assessed using Receiver Operating Characteristic (ROC) analysis, measuring sensitivity, specificity, positive predictive value (PPV), negative predictive value (NPV), and accuracy, with a significance level set at $p < 0.05$.

In conclusion, this methodical approach aimed to provide comprehensive insights into the utility of DW-MRI and ADC values for differentiating benign and malignant cervical lymph nodes, potentially enhancing diagnostic accuracy and patient care.

RESULT

In our observational study, the age range of participants varied significantly from 17 to 96 years, with the highest incidence observed in the fifth decade of life (Table 1).

Table 1: Distribution of Subjects based on Age Groups

Age group	Frequency	Percent
Upto 20 yrs	4	8.5
21 - 30 yrs	5	10.6
31 - 40 yrs	8	17.0
41 - 50 yrs	6	12.8
51 - 60 yrs	10	21.3
61 - 70 yrs	8	17.0
71 - 80 yrs	4	8.5
Above 80 yrs	2	4.3
Total	47	100.0

The study population consisted of 63.8% males and 36.2% females (Table 2).

Table 2: Distribution of Subjects based on Gender

Gender	Frequency	Percent
Female	17	36.2
Male	30	63.8
Total	47	100.0

Based on histopathological examination (HPE) diagnoses, 51.1% of cases were identified as benign, while 48.9% were malignant (Table 3).

Table 3: Nature of the Lesion based on HPE

	Frequency	Percent
Malignant	23	48.9
Benign	24	51.1
Total	47	100.0

The predominant causes of cervical lymphadenopathy in our study were metastasis (40.4%), lymphoma (8.5%), and benign lymphadenopathy (51.1%) (Figure 1).

HPE Diagnosis

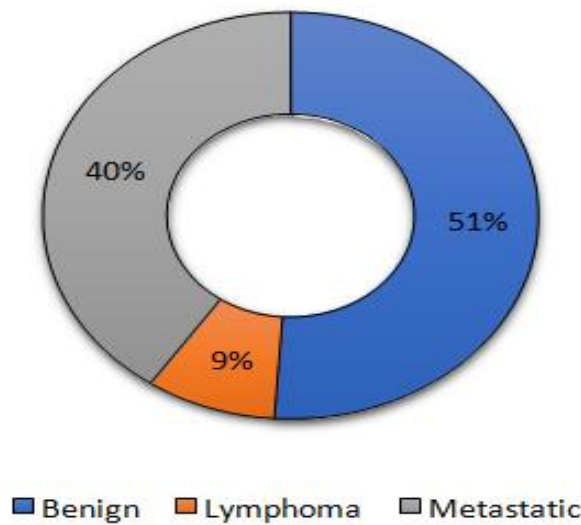


Figure 1: Distribution of Subjects based on HPE Diagnosis

Among benign nodes, reactive lymphoid hyperplasia accounted for 50%, kikuchi lymphadenitis for 4.1%, and tuberculous lymphadenitis for 45.9% (Figure 2).

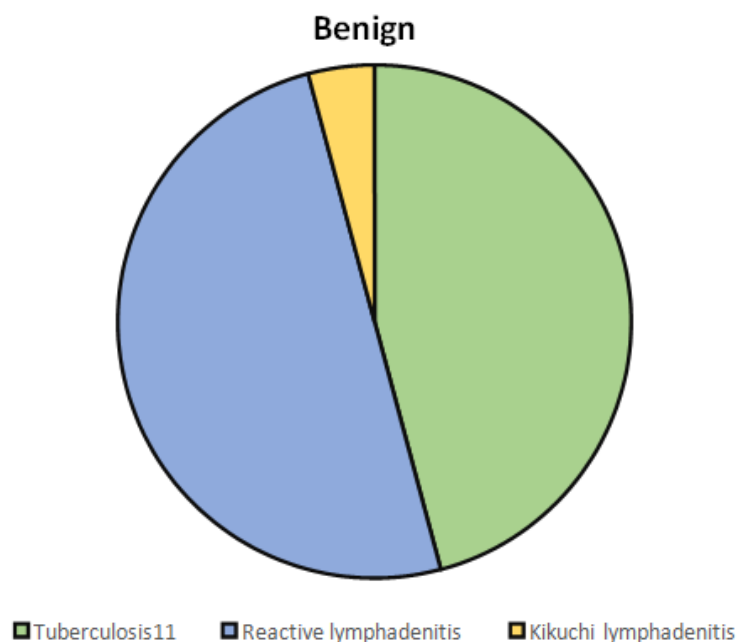


Figure 2: Causes of Benign Lymphadenopathy

Metastatic lymph nodes originated predominantly from moderately differentiated squamous cell carcinoma (47.3%) and poorly differentiated squamous cell carcinoma (42.1%), followed by medullary carcinoma of the thyroid (5.2%) and small cell carcinoma of the lung (5.2%) (Figure 3).

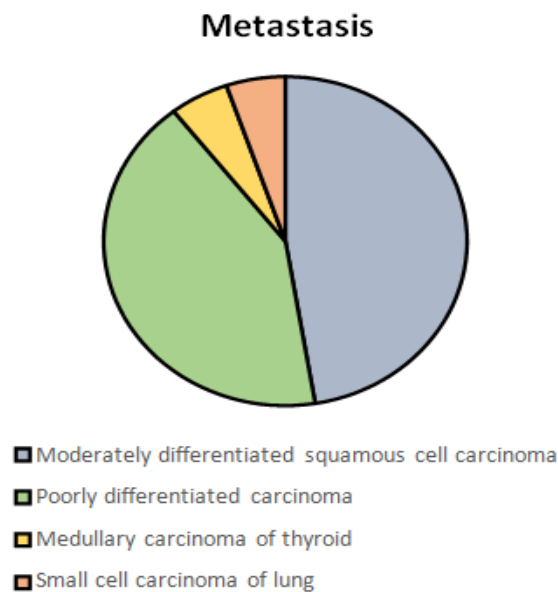


Figure 3: Causes of Metastatic Lymphadenopathy

Lymphomatous nodes were equally divided between non-Hodgkin lymphoma (NHL) and Hodgkin lymphoma (HL), each comprising 50%. The mean ADC values were obtained for all the benign and malignant lesions (Table 4).

Table 4: Causes and Mean ADC Values of Cervical Lymphadenopathy

Pathology	Number	Mean ADC value
Metastasis		
Moderately differentiated carcinoma	9	0.82+/-0.11 x 10 ⁻³ mm ² /s
Poorly differentiated carcinoma	8	0.72+/-0.08 x 10 ⁻³ mm ² /s
Medullary carcinoma of thyroid	1	0.61 x 10 ⁻³ mm ² /s
Small cell carcinoma of lung	1	0.82 x 10 ⁻³ mm ² /s
Lymphomatous		
NHL	2	0.70+/-0.06 x 10 ⁻³ mm ² /s
HL	2	0.67+/-0.11 x 10 ⁻³ mm ² /s
Benign		
Tuberculosis	11	1.08+/-0.12 x 10 ⁻³ mm ² /s
Reactive lymphadenitis	12	1.14+/-0.17 x 10 ⁻³ mm ² /s
Kikuchi lymphadenitis	1	0.99 x 10 ⁻³ mm ² /s

Statistical analysis revealed a highly significant difference between ADC values and HPE diagnoses. The Independent sample t-test yielded a t-value of 9.280 and a p-value of 0.0005<0.01, indicating a strong statistical significance (Table 5).

Table 5: Comparison of ADC with HPE by Independent Sample T-test

Variable	HPE	N	Mean	SD	t-value	p-value
ADC	Malignant	23	.75	.11	9.280	0.0005 **
	Benign	24	1.11	.15		
** Highly Statistical Significance at p < 0.01 level						

Similarly, the Receiver Operating Characteristic (ROC) analysis demonstrated an area under the curve of 0.972 with a p-value of 0.0005<0.01 and a 95% confidence interval ranging from 0.930 to 1.000 (Table 6).

Table 6: Comparison of ADC with HPE Diagnosis using Receiver Operating Characteristic Curve (ROC)

Area	Std. Error ^a	p-value	95% C.I	
			LB	UB
.972	.022	0.0005 **	.930	1.000
** Highly Statistical Significance at p < 0.01 level				

This analysis showed a sensitivity of 95.7%, specificity of 91.7%, positive predictive value (PPV) of 97.1%, negative predictive value (NPV) of 95.7%, and an overall accuracy of 93.6% (Table 7).

Table 7: ADC and HPE Diagnosis Cross Tabulation

		HPE		Total	Sensitivity	95.7
		Malignant	Benign		Specificity	91.7
ADC	<= 0.95	22	2	24	PPV	91.7
	> 0.95	1	22	23	NPV	95.7
Total		23	24	47	Accuracy	93.6

Furthermore, Pearson's Chi-Square test also confirmed a highly significant association between ADC values and HPE diagnoses, with a χ^2 value of 1.289 and a p-value of 0.0005<0.01 (Table 8).

Table 8: Comparison of ADC with HPE by Pearson's Chi-Square Test

ADC		HPE		Total	χ^2 -value	p-value
		Malignant	Benign			
0.5 - 0.59	Count	2	0	2	35.449	0.0005 **
	%	8.7%	0.0%	4.3%		
0.6 - 0.69	Count	5	0	5		
	%	21.7%	0.0%	10.6%		
0.7 - 0.79	Count	10	0	10		
	%	43.5%	0.0%	21.3%		
0.8 - 0.89	Count	3	1	4		
	%	13.0%	4.2%	8.5%		
0.9 - 0.99	Count	2	9	11		
	%	8.7%	37.5%	23.4%		
1 - 1.09	Count	1	1	2		
	%	4.3%	4.2%	4.3%		
1.1 - 1.19	Count	0	3	3		
	%	0.0%	12.5%	6.4%		
1.2 - 1.29	Count	0	7	7		
	%	0.0%	29.2%	14.9%		
1.3 - 1.39	Count	0	3	3		
	%	0.0%	12.5%	6.4%		
TOTAL	Count	23	24	47		
	%	100.0%	100.0%	100.0%		

In conclusion, our study underscores the potential of ADC values derived from DW-MRI as a reliable tool for distinguishing between benign and malignant cervical lymph nodes, offering high sensitivity, specificity, and overall accuracy in diagnostic evaluations. In our study, Figure 4 illustrates a tubercular cervical lymph node, as depicted in the axial T2W MR image (A), which shows an enlarged right level II lymph node with mixed signal intensity (SI). The same lymph node exhibits high SI on DW-MRI images at b=0 s/mm² (B) and b=1,000 s/mm² (C), and mixed SI on the ADC map (D). The mean ADC value for this lymph node was calculated to be 1.03±0.23x10⁻³ mm²/s.

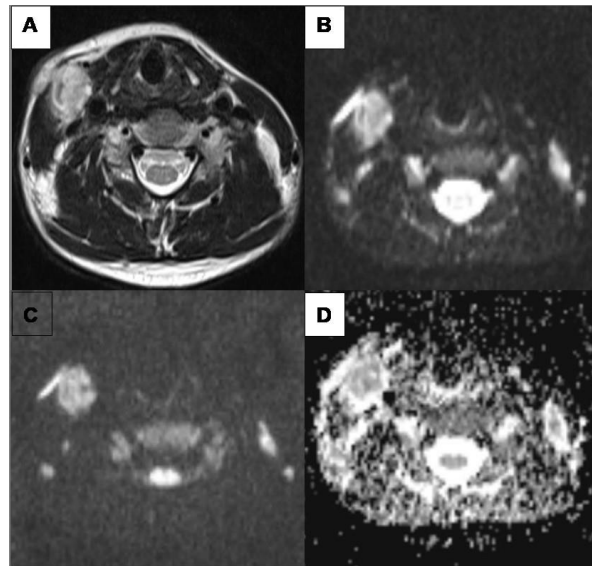


Figure 4: Tubercular cervical lymph node. Axial T2W MR image (A) showing enlarged right level II lymph node with mixed SI. Enlarged right level II lymph node show high SI on DW-MRI image at $b=0$ s/mm² (B) and $b=1,000$ s/mm² (C). Enlarged right level II lymph node shows mixed SI on ADC map (D). The mean ADC value of the right level II lymph node is $1.03 \pm 0.23 \times 10^{-3}$ mm²/s

Similarly, Figure 5 showcases a case of NHL. The axial T1W MR image (A) displays multiple enlarged left level II lymph nodes with homogeneously low SI. These enlarged lymph nodes present high SI on DW-MRI images at $b=0$ s/mm² (B) and $b=1,000$ s/mm² (C), while showing low SI on the ADC map (D). The mean ADC value for the left level II lymph node in this case was $0.65 \pm 0.11 \times 10^{-3}$ mm²/s.

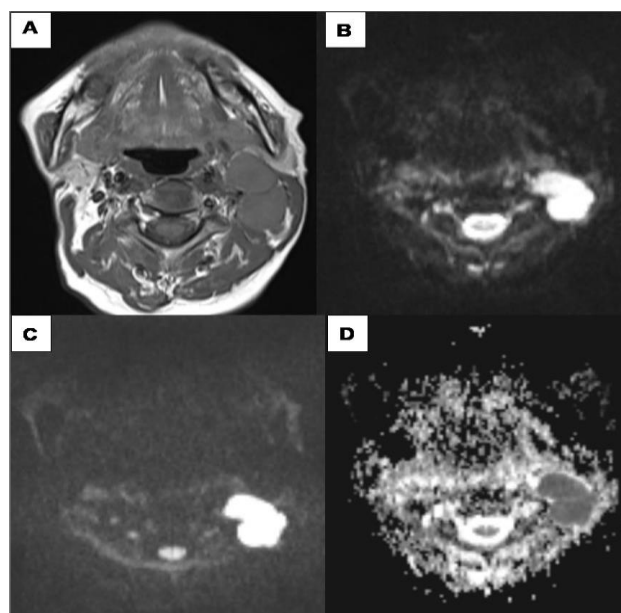


Figure 5: NHL. Axial T1W MR image (A) showing multiple enlarged left level II lymph nodes with homogeneously low SI. Enlarged lymph nodes show high SI on DW-MRI image at $b=0$ s/mm² (B) and $b=1,000$ s/mm² (C). Enlarged lymph nodes shows low SI on ADC map (D). The mean ADC value of the left level II lymph node is $0.65 \pm 0.11 \times 10^{-3}$ mm²/s

DISCUSSION

The random movement of water molecules in a solution is referred as diffusion. Robert Brown (1773-1858) was the first to describe this phenomenon. After him, this phenomenon was named "Brownian motion" [1]. Following Bloch and Purcell's [2,3] first description of the Nuclear Magnetic Resonance (NMR) effect in 1946, four years later the sensitivity of the technique for molecular diffusion processes was marked in Hahn's publication [4] on spin echoes. Carr and Purcell [5] investigated the details further in 1954. Stejskal and Tanner [6] published an early description of a diffusion weighted (DW) sequence for measuring the diffusion properties of a substrate in 1965.

Lauterbur's [7] ground-breaking publication in 1973 described the principles of NMR imaging using the back-projection technique. After that, it took another 12 years to combine imaging and diffusion. Taylor and Bushel were the first to describe DW-MRI [8].

Cervical node examination plays a pivotal role in diagnosing and staging malignant conditions, as well as in planning therapy and follow-up. Despite advancements in imaging techniques such as contrast-enhanced MRI, CT, and ultrasound, achieving optimal accuracy remains a challenge. Ultrasound-guided fine-needle aspiration cytology (FNAC) has proven reliable but is operator-dependent, invasive, and has a notable rate of false-negative results [9].

Diffusion-weighted MRI (DW-MRI) emerges as a non-invasive technique capable of measuring water movement in extracellular spaces, with cellularity being the primary limiting factor for water diffusion. Malignant conditions, characterized by increased cell density, nucleocytoplasmic ratio, and reduced extracellular space, hinder water diffusion, reflected in reduced ADC values on DW-MRI. The ADC map, quantifying water diffusion, enables precise tissue characterization and has shown potential to enhance diagnostic accuracy in differentiating benign from malignant nodes [10].

Our observational study, conducted over 18 months at a tertiary care hospital included 47 subjects with lymphadenopathy. MRI sequences with DW and conventional sequences were employed, and ADC values were correlated with histopathological examination (HPE) as the gold standard.

Participants ranged from 17 to 96 years, with the elderly age group being the most common demographic. The male-to-female ratio was approximately 2:1. HPE confirmed 51.1% benign and 48.9% malignant lymph nodes. Mean ADC values were significantly lower in malignant ($0.75 \pm 0.11 \times 10^{-3} \text{ mm}^2/\text{s}$) than benign nodes ($1.11 \pm 0.15 \times 10^{-3} \text{ mm}^2/\text{s}$). Furthermore, ADC values varied with metastatic node differentiation; poorly differentiated nodes had lower ADC values ($0.72 \pm 0.08 \times 10^{-3} \text{ mm}^2/\text{s}$) than moderately differentiated nodes ($0.82 \pm 0.11 \times 10^{-3} \text{ mm}^2/\text{s}$).

Comparing our findings with previous studies, consistent trends were observed. Tamer F. Taha Ali [9] found significantly lower ADC values in metastatic ($0.92 \times 10^{-3} \text{ mm}^2/\text{s}$) versus benign nodes ($1.51 \times 10^{-3} \text{ mm}^2/\text{s}$), whereas NHL had lower ADC values ($0.65 \times 10^{-3} \text{ mm}^2/\text{s}$) than HL ($0.86 \times 10^{-3} \text{ mm}^2/\text{s}$). Our study showed similar but slightly varied ADC values, with NHL ($0.70 \times 10^{-3} \text{ mm}^2/\text{s}$) slightly higher than HL ($0.67 \times 10^{-3} \text{ mm}^2/\text{s}$).

Turgut Seber et al. [10] reported higher mean ADC values for benign ($0.97 \times 10^{-3} \text{ mm}^2/\text{s}$) versus malignant ($0.76 \times 10^{-3} \text{ mm}^2/\text{s}$) nodes, with a cut-off of $0.8 \times 10^{-3} \text{ mm}^2/\text{s}$. Our study aligns with these findings, but our cut-off ADC value was slightly

higher ($0.95 \times 10^{-3} \text{ mm}^2/\text{s}$). Ahmed Abdel et al. [11] and PerroneA et al. [12] also reported significantly lower ADC values in metastatic and lymphomatous nodes compared to benign nodes, with cut-off values slightly higher or lower than our study, respectively.

Our findings corroborate studies by K. Holzapfel et al. [13] and Guan Qiao Jin et al. [14], where malignant nodes had significantly lower ADC values than benign nodes. F. Tondo et al. [15] proposed a higher ADC threshold ($1.25 \times 10^{-3} \text{ mm}^2/\text{s}$) to differentiate malignant and benign nodes.

Alamolhoda et al [16] in 2016 studied the DWI of Neck lymph nodes. In the study about Sixty-five patients with head and neck lesions were included (71 benign, 40 malignant). Statistically significant differences ($p < 0.001$) were seen in the mean ADC values \pm SD of malignant and benign lesions ($0.55 \times 10^{-3} \pm 0.14 \times 10^{-3} \text{ mm}^2/\text{s}$ vs $0.89 \times 10^{-3} \pm 0.29 \times 10^{-3} \text{ mm}^2/\text{s}$, respectively) and in the mean ADC ratios of malignant and benign lesions (0.88 ± 0.21 vs 1.40 ± 0.44 , respectively).

Noha Abd ElShafy ElSaid et al. (2014) [17] found significant differences in mean ADC values between benign and malignant cervical lymph nodes. Miller et al [18] Polat Kosucu MD et al. (2009) [19] determined that DW-MRI with ADC values and signal intensity effectively distinguished between benign and malignant mediastinal lymph nodes. Additionally, Hiroki Kato et al. (2013) [20] and Guan Qiao Jin, MD et al. (2016) [21] highlighted the utility of DWI and ADC values in differentiating between various lymph node pathologies and malignancies, supporting the diagnostic value of our identified ADC threshold.

Importantly, our study identified an ADC value threshold of $< 0.8 \times 10^{-3} \text{ mm}^2/\text{s}$ on DWI as indicative of a higher likelihood of malignancy. This threshold demonstrated 95.7% sensitivity, 91.7% specificity, 91.7% positive predictive value (PPV), and 95.7% negative predictive value (NPV), with an overall accuracy of 93.6%.

However, MR imaging artifacts can affect ADC measurements, necessitating methods to minimize distortion and enhance signal-to-noise ratio for improved accuracy. Despite these challenges, our study's statistically significant findings ($p \leq 0.01$) support the potential of DW-MRI in enhancing diagnostic precision for cervical lymphadenopathy.

In conclusion, our study underscores the utility of DW-MRI and ADC values in distinguishing between benign and malignant cervical lymph nodes. The identified ADC threshold of $< 0.8 \times 10^{-3} \text{ mm}^2/\text{s}$ demonstrates high sensitivity and specificity, potentially reducing the need for invasive diagnostic procedures. Future research focusing on reducing imaging artifacts and optimizing DW-MRI techniques could further enhance diagnostic accuracy and clinical utility in cervical lymphadenopathy management.

CONCLUSION

DW-MRI with ADC mapping is a promising technique that can differentiate malignant from benign lymph nodes. DWI can be preferred as a non-invasive method for patients with enlarged cervical lymph nodes enabling earlier diagnosis and treatment planning.

Limitations of the Study

The limitation in our study was because of the low spatial resolution of echoplanar imaging that worsens using high b values ($b = 1000 \text{ s/mm}^2$), that on the other hand are necessary to improve the sensitivity of diffusion imaging. For this reason the small nodes with a diameter inferior to 9 mm are difficult to detect on ADC maps.

Acknowledgment

The authors acknowledge the patients as a great source of learning.

Declaration of Consent

The authors attest that they have all the necessary permissions in place to publish this original article.

Competing Interests

The authors claim they have no competing interests, either financial or non-financial.

Financial Support and Sponsorship

The authors state that sponsorship was secured for this study and that they do not receive any funding.

Declaration of Generative AI and AI-assisted Technologies in the Writing Process:

During the preparation of this work, OpenAI was used in order to improve language and readability. After using this tool/service, the author(s) reviewed and edited the content as needed and take full responsibility for the content of the publication.

References

- 1) Kerker M. Brownian movement and molecular reality prior to 1900. J Chem Educ. 1974 Dec 1;51(12):764
- 2) Bloch F, Hansen WW, Packard M. Nuclear Induction. Phys Rev 1946;69:127134.
- 3) Purcell EM, Torrey HC, Pound RV. Resonance absorption by nuclear magnetic moments in a solid. Phys Rev 1946;69:37
- 4) Hahn EL. Spin echoes. Phys Rev 1950;80:580-94.
- 5) Carr HY, Purcell EM. Effects of free precession in nuclear magnetic resonance experiments. Phys Rev 1954;94:630-38.
- 6) Stejskal EO, Tanner JE. Spin diffusion measurements: spin echoes in the presence of a time-dependent field gradient. The journal of chemical physics. 1965 Jan 1;42(1):288-92.
- 7) Lauterbur PC. Image formation by induced local interactions: examples employing nuclear magnetic resonance. Nature 1973;242:190-91.
- 8) Taylor DG, Bushell MC. The spatial mapping of translational diffusion coefficients by the NMR imaging technique. Physics in Medicine and Biology 1985;30:345-49.
- 9) Taha Ali TF. Neck lymph nodes: Characterization with diffusion-weighted MRI. Egypt J Radiol Nucl Med. 2012 Jun 1;43(2):173–81.
- 10) Seber T, Caglar E, Uylar T, Karaman N, Aktas E, Aribas BK. Diagnostic value of diffusion-weighted magnetic resonance imaging: differentiation of benign and malignant lymph nodes in different regions of the body. Clin Imaging. 2015 Oct;39(5):856–62.
- 11) Abdel Razek AAK, Soliman NY, Elkhamary S, Alsharaway MK, Tawfik A. Role of diffusion-weighted MR imaging in cervical lymphadenopathy. Eur Radiol. 2006 Jul;16(7):1468–77.
- 12) Perrone A, Guerrisi P, Izzo L, D'Angeli I, Sassi S, Mele LL, Marini M, Mazza D, Marini M. Diffusion-weighted MRI in cervical lymph nodes: differentiation between benign and malignant lesions. European journal of radiology. 2011 Feb 28; 77(2):281-6.
- 13) Holzapfel K, Duetsch S, Fauser C, Eiber M, Rummeny EJ, Gaa J. Value of diffusion-weighted MR imaging in the differentiation between benign and malignant cervical lymph nodes. Eur J Radiol. 2009 Dec;72(3):381–7.

- 14) Jin GQ, Yang J, Liu LD, Su DK, Wang DP, Zhao SF, Liao ZL. The diagnostic value of 1.5-T diffusion-weighted MR imaging in detecting 5 to 10 mm metastatic cervical lymph nodes of nasopharyngeal carcinoma. *Medicine*. 2016 Aug;95(32):e4286.
- 15) Tondo F, Saponaro A, Stecco A, Lombardi M, Casadio C, Carriero A. Role of diffusion-weighted imaging in the differential diagnosis of benign and malignant lesions of the chest-mediastinum. *Radiol med* 2011; 116:720-33.
- 16) Alamolhoda F, Faeghi F, Bakhshandeh M, Ahmadi A, Sanei Taheri M, Aabbasi S. Diagnostic Value of Diffusion Weighted Magnetic Resonance Imaging in Evaluation of Metastatic Neck Lymph Nodes in Head and Neck Cancer: A Sample of Iranian Patient. *Asian Pac J Cancer Prev*. 2019 Jun 1;20(6):1789-1795.
- 17) ElSaid NA, Nada OM, Habib YS, Semeisem AR, Khalifa NM. Diagnostic accuracy of diffusion weighted MRI in cervical lymphadenopathy cases correlated with pathology results. *The Egyptian Journal of Radiology and Nuclear Medicine*. 2014 Dec 31; 45(4):1115-25.
- 18) Miller F H, Hammond N, Siddiqi A J, Shroff S, Khatri G, Wang Y et al. Utility of Diffusion-Weighted MRI in Distinguishing Benign and Malignant Hepatic Lesions. *J Magn Reson Imaging* 2010; 32: 138-47.
- 19) Kosucu P, Tekinbas C, Erol M, Sari A, Kavgaci H, Oztuna F et al, Mediastinal Lymph Nodes: Assessment With Diffusion –Weighted MR Imaging. *J Magn Reson Imaging* 2009; 30:292-7.
- 20) Kato H, Kanematsu M, Kato Z, Teramoto T, Mizuta K, Aoki M, Makita H, Kato
- 21) K. Necrotic cervical nodes: usefulness of diffusion-weighted MR imaging in the differentiation of suppurative lymphadenitis from malignancy. *European journal of radiology*. 2013 Jan 31; 82(1): e28-35.
- 22) Jin GQ, Yang J, Liu LD, Su DK, Wang DP, Zhao SF, Liao ZL. The diagnostic value of 1.5-T diffusion-weighted MR imaging in detecting 5 to 10 mm metastatic cervical lymph nodes of nasopharyngeal carcinoma. *Medicine*. 2016 Aug;95(32):e4286.